Journal of Bioenergetics and Biomembranes, Vol. 24, No. 1, 1992

Research Paper

Binding of a Synthetic Targeting Peptide to a Mitochondrial Channel Protein

Carmen A. Mannella,[1,2] Xiao Wei Guo,[1] and James Dias[1,2]

Received May 15, 1991; revised July 1, 1991

Membrane crystals of the mitochondrial outer membrane channel VDAC (porin) from *Neurospora crassa* were incubated with a 20-amino-acid synthetic peptide corresponding to the N-terminal targeting region of subunit IV of cytochrome oxidase. The peptide caused disordering and contraction of the crystal lattice of the membrane arrays. Also, new stain-excluding features were observed on the peptide-treated arrays which most likely correspond to sites at which the peptide accumulates. The stain exclusion zones associated with binding of the targeting peptide (and with binding of apocytochrome *c* in an earlier study) have been localized on a two-dimensional density map of frozen-hydrated, crystalline VDAC previously obtained by cryo-electron microscopy. The results indicate that both the peptide and cytochrome *c* bind to protein "arms" which extend laterally between the channel lumens. The finding that imported polypeptides bind to a specific region of the VDAC protein implicates this channel in the process by which precursor proteins are recognized at and translocated across the mitochondrial outer membrane.

KEY WORDS: Mitochondrial channels; mitochondrial targeting sequences; electron microscopy; computer image processing.

INTRODUCTION

Most of the proteins comprising the mitochondrion are encoded by nuclear DNA and synthesized on cytoplasmic ribosomes. The mechanisms by which proteins destined for incorporation into the mitochondrion are recognized at this organelle's surface and subsequently transported across one or both of its membranes are under intense study but are not as yet fully defined (e.g., Hartl *et al.*, 1989; Baker and Schatz, 1991). There is considerable evidence which suggests that the recognition process involves the segments of 20 or more residues which are cleaved from the amino termini of imported proteins in the course of their uptake by mitochondria (Roise, 1988). While the N-terminal "targeting" regions of different mitochondrial proteins are not generally homologous, they are all predicted to form positively charged, amphiphilic α-helices (von Heijne, 1986). There is good evidence that the targeting function of these peptides correlates with their tendency to form amphiphilic helices (Roise, 1988; Roise *et al.*, 1988; Lemire *et al.*, 1989).

One of several open questions concerning protein translocation across mitochondrial membranes is whether it occurs via pre-existing channels or pores. There are two indirect pieces of evidence favoring the involvement of channels in the process of mitochondrial protein uptake. First, there is the observation by Mannella *et al.* (1987) and Mannella (1989) that apocytochrome *c* binds to a site on the periphery of the mitochondrial outer membrane channel, VDAC (voltage-dependent, anion-selective channel; see Colombini, 1979; also called mitochondrial porin;

[1]Wadsworth Center for Laboratories and Research, New York State Department of Health, Empire State Plaza, Albany, New York 12201-0509.

[2]Department of Biomedical Sciences, School of Public Health, State University of New York at Albany, Albany, New York 12201-0509.

0145-479X/92/0200-0055$06.50/0

see Benz, 1985). Second, Henry *et al.*, (1989) have found that a large channel which they reconstitute from mitochondria is blocked by a synthetic peptide with the sequence of a targeting region of an imported protein.

Of all the mitochondrial channels detected to date, VDAC is the best characterized both functionally and structurally. When reconstituted in phospholipid bilayers, it displays a high-conductance open state (ca. 4 nS in 1 M KCl) which is switched or gated to less conducting substates by transmembrane potentials of 20–30 mV (Colombini, 1979; Benz, 1985). This gating potential is substantially decreased by macromolecular modulators which include a synthetic polyanion (Colombini *et al.*, 1987) and an endogenous mitochondrial protein (Holden and Colombini, 1988). The 30-kDA VDAC protein forms periodic arrays in mitochondrial outer membranes of the fungus *Neurospora crassa* when these membranes are slowly depleted of lipid by phospholipase A_2 (Mannella, 1984, 1986; Mannella *et al.*, 1986). Electron microscopy of negatively stained and unstained, frozen-hydrated membrane arrays indicate that the VDAC protein forms a large, water-filled pore with a lumen diameter of approximately 2.5 nm (Mannella *et al.*, 1986, 1989). The crystalline arrays of VDAC are polymorphic, i.e., they may have more than one kind of lattice geometry. The usual unit cell is a parallelogram (13.3 nm × 11.5 nm, lattice angle 109°) holding six VDAC channels. Other crystal types are also observed in which the lattice angle is reduced and the repeat units of six VDAC channels are more closely packed. These "contracted" polymorphs are normally found only in mitochondrial outer membrane fractions after extensive phospholipase treatment (Mannella, 1986). However, the modulator polyanion has been found to trigger rapid contraction of the parellelogram VDAC lattice (Mannella and Guo, 1990).

VDAC occurs at surface densities of 10^3 to 10^4 per square μm on native outer membranes of fungal and animal mitochondria (Freitag *et al.*, 1982; DePinto *et al.*, 1987); $4 \times 10^4/\mu m^2$ in the phospholipase-induced periodic arrays of *Neurospora*. The ubiquity of this channel, its large lumen diameter, and its high density at the mitochondrial surface raise the question of whether it might be involved in protein recognition and/or translocation at the mitochondrial outer membrane. As one approach to this question, we have used electron microscopy and image processing to study the interactions between this channel and imported proteins (e.g., the cytochrome *c* binding study noted above). In the present report, we describe structural changes induced in membrane crystals of the VDAC protein by a synthetic peptide corresponding to the N-terminal targeting sequence of subunit IV of *Neurospora* cytochrome oxidase. The sites at which this peptide binds are localized on a two-dimensional density map of the channel crystals (previously provided by cryo-electron microscopy). These targeting-peptide binding sites are compared with those previously identified for apo-cytochrome *c*. The results indicate that both the presequence and the imported protein bind to the same region on the channel protein.

MATERIALS AND METHODS

The peptide corresponding to amino acids 3–22 of subunit IV of *Neurospora* cytochrome oxidase, (R A P A L R R S I A T T V V R C N A E T; see Sachs *et al.*, 1986) was synthesized utilizing Fmoc chemistry on an Applied Biosystems (Foster City, California) 431A automated peptide synthesizer. Standard cycles were used, with an HMP resin and a fourfold molar excess of activated amino acid. Peptides were cleaved from the resin and deprotected by standard procedures (trifluoroacetic acid with ethanedithiol and anisole as scavengers). The cleavage product was extracted twice with cold diethyl ether and dissolved in 1 M acetic acid, then the product was lyophilized. The final product was about 50% peptide by mass, the rest being acetate salts. HPLC analysis indicated the existence of monomer and dimer peptides, the dimers formed by oxidation of Cys18 residues. Amino acid compositional analysis of the monomer peptides (determined using a Beckman Systems Gold amino acid analyzer with ninhydrin analysis) confirmed the expected molar equivalents of each amino acid. The sequence of the peptide was subsequently confirmed using an Applied Biosystems 477A peptide sequencer.

Membrane crystals of VDAC were made by phospholipase A_2 treatment of outer membranes isolated from *Neurospora* mitochondria, as described elsewhere (Mannella, 1984, 1986; Mannella *et al.*, 1986). The membranes (approximately 0.2 mg protein per ml of low-salt buffer, containing 10 mM Tris-HCl, 0.25 mM sodium EDTA, pH 7) were mixed with equal aliquots of low-salt buffer containing 0, 10, 100 or 200 μM peptide. (The results described below were equivalent whether peptide fractions containing monomers and dimers or HPLC-purified monomers

were used. Also, the results were independent of pH in the range 5–7.) After 1-hour incubation at room temperature, 5–10-μl aliquots of the peptide–membrane mixtures were deposited on glow-discharged, carbon-coated, copper specimen grids, mixed with equal volumes of either 1% uranyl acetate (pH 4.3) or 1% aurothioglucose (pH 7.0), and allowed to dry. These "negatively stained" specimens were examined in a Philips EM420-T electron microscope (Philips Electronic Instruments, West Nyack, New York) operated at 100 kV and images were recorded on Kodak SO-163 film (Eastman Kodak, Rochester, New York). Low-dose imaging conditions (Mannella *et al.*, 1986) were used with aurothioglucose-embedded membranes.

Optical diffraction (using a He–Ne laser, Jodon Engineering Associates, Ann Arbor, Michigan) was used to determine the lattice type and degree of order of the crystals in the different specimens. Average projection images were computed from selected crystals by quasioptical Fourier filtration (Goldfarb *et al.*, 1979) and correlation averaging (Saxton, 1980; Frank, 1982) as described in detail elsewhere (Mannella *et al.*, 1986; Mannella and Guo, 1990), using the SPIDER image processing system (Frank *et al.*, 1981) implemented on a VAXstation 3500 (Digital Equipment Corp, Maynard, Massachusetts). Briefly, in quasioptical filtration, the Fourier transform of an image is computed and a mask is made (by an interactive lattice refinement method) which includes only those components in the transform which fall on the reciprocal lattice of one planar crystalline layer. Inverse transformation of the masked transform yields a two-dimensional average of that crystal layer. The Fourier-averaged unit cell is used as a reference for cross-correlating with the entire crystal field. Maxima in the resulting cross-correlation function indicate the precise positions of best agreement between the image and reference. Summation of subfields windowed from the image at these loci yields so-called correlation averages. Since this process corrects for lattice disorder, correlation analysis can yield averages with better resolution than those obtained by quasioptical Fourier filtration alone.

RESULTS

Effects of the Targeting Peptide on VDAC Membrane Crystals

Membrane crystals of the VDAC protein, made by phospholipase A_2 treatment of outer membranes of fungal mitochondria, were incubated with a synthetic peptide corresponding to the N-terminal region of fungal cytochrome oxidase subunit IV (Sachs *et al.*, 1986). The final concentrations of peptide used (5 and 100 μM) bracket the range commonly used in *in vitro* studies of the effects of targeting peptides on mitochondrial protein import (e.g., Glaser and Cumsky, 1990).

The morphology and substructure of membrane crystals of the VDAC channel are typified by the membrane of Fig. 1A. It is a collapsed tube or cylinder, 0.4 μm wide and over 0.5 μm in length. Figure 1C is the computed diffraction pattern (Fourier power spectrum) for a 0.12 μm square region near the center of the membrane. The sharp maxima fall on two superimposed planar parallelogram lattices, related by mirror symmetry and a slight rotation. This diffraction pattern is characteristic of the flattened cylindrical arrays formed by VDAC in phospholipase-treated outer mitochondrial membranes (Mannella, 1984; Mannella *et al.*, 1986). An image of a single array layer in the collapsed tubular membrane of Fig. 1A (obtained by quasioptical Fourier filtration) is presented in Fig. 1D. The lattice direction designated as **b** runs nearly parallel to the long axis of the membrane tube, with the **a** vector taking off at an angle of 108° with respect to **b**. The repeating unit is a group of six channels, whose lumens appear dark because they are filled with negative stain (in this case, uranyl acetate).

There are no obvious differences in the morphology of VDAC membrane crystals treated with the lower concentration of peptide (5 μM). However, incubation of the membrane crystals with 50 or 100 μM peptide results in several marked changes in their appearance and substructure. First and most obvious, the peptide-treated membranes are coated with patches of stain-excluding (white) fibers or filaments. There is considerable variability in the size and shape of these threadlike features, which are 1 or 2 nm thick and several nm in length. Similar structures are not seen in images of control VDAC arrays, suggesting that the fibers represent aggregates of the targeting peptide itself. While the fibers generally appear to be arranged randomly on the membranes, some membrane regions show evidence of periodic decoration by the peptide. A striking example is provided in Fig. 1B, a membrane crystal similar in size and shape to that of Fig. 1A but which has a distinct pattern of white stripes running parallel to the long axis of the membrane tube (i.e., the **b** lattice direction).

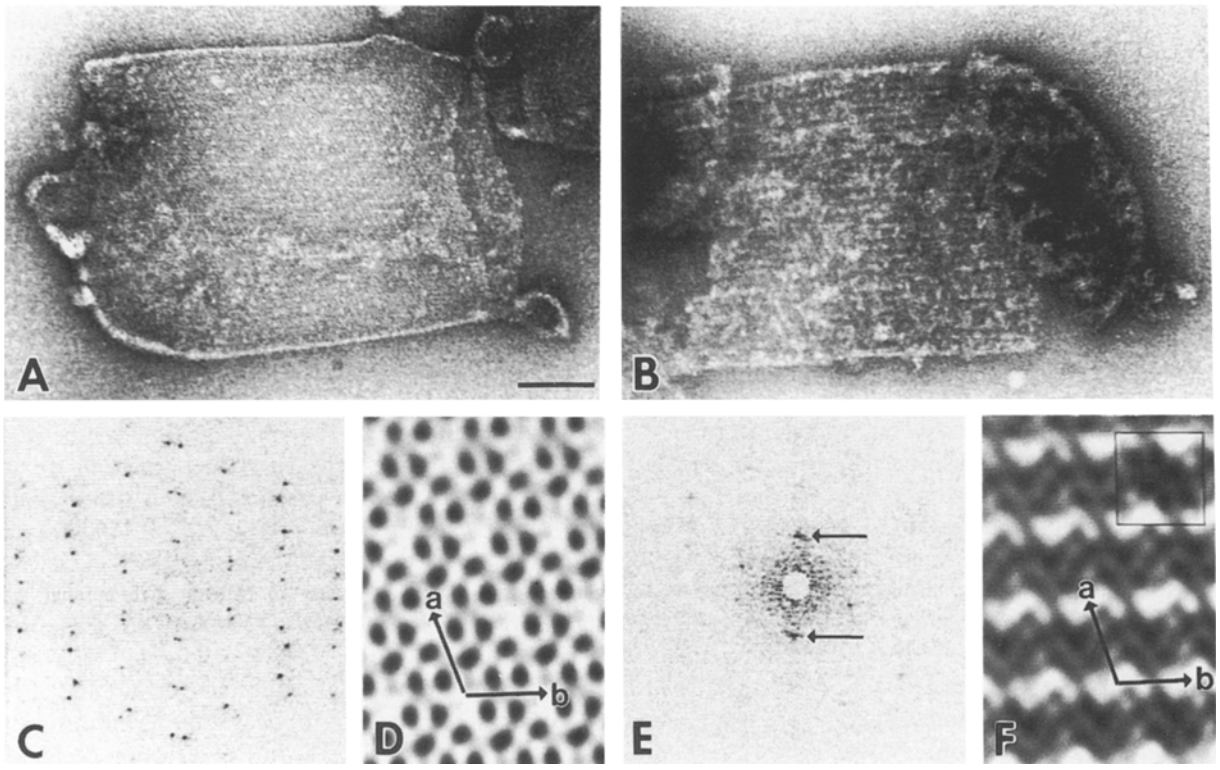

Fig. 1. Effect of the cytochrome oxidase targeting peptide on the structure of membrane crystals of the VDAC channel from *N. crassa* mitochondria. (A,B) Electron micrographs of control (A) and + peptide (B) VDAC arrays negatively stained with uranyl acetate. Bar = 100 nm. (C,E) Computed diffraction patterns from 115 nm square regions at the upper central region in the crystals of (A) and (B), respectively. Arrows in (E) point to the (1,0) and (−1,0) reflections at about 1/(13 nm). (D,F) Fourier filtration of the regions corresponding to the diffraction patterns in (C) and (E), respectively. Unit cell vectors are indicated in both cases. The inset in (F) is a correlation average of a single crystal layer from a field in (B) just to the left of that from which the Fourier average of (F) was computed.

Such striated patterns suggest a specificity in the attachment of the peptide to the membrane arrays.

In contrast with optical and computed diffraction patterns from control membranes (e.g. Fig. 1C), those from peptide-treated membrane crystals generally contain weak, diffuse maxima, indicating that the arrays have poor long-range order. In regions of peptide-treated membranes from which interpretable diffraction maxima could be recorded, the lattice parameters indicate that contraction of the VDAC arrays had occurred (see Introduction), with lattice angles falling in the range 104–98°. The example of Fig. 1B was chosen in part because it was the least contracted peptide-treated array (lattice angle 104°) from which a usable diffraction pattern could be obtained (Fig. 1E). The strongest features in the computed diffraction pattern from this membrane crystal are the reflections at about 1/(13 nm), corresponding to the reciprocal of the spacing between adjacent white stripes in the membrane image. In the average obtained by Fourier filtration of the corresponding region of the peptide-treated membrane (Fig. 1F), the white stripes are resolved as parallel rows of white "s"-shaped features. The pronounced striping observed in regions such as these apparently results when the lattices of the two apposed layers in a collapsed tubular membrane are partly "in register," i.e., the rows of pores running parallel to the **b** lattice direction in each layer coincide in projection. While this coincidence enhances the white featues aligned along the **b** direction in the arrays, it has the consequence that the images of the top and bottom layers cannot be completely separated in these regions. As a result, the repeat unit of six pores is difficult to distinguish in the Fourier average of Fig. 1F. Fortunately, the two apposed lattices in an adjacent region of the same membrane crystal were sufficiently out of register to allow separate reconstruction of each layer. The corresponding correlation average of a unit cell from one array layer, showing six distinguishable pores, is shown in the inset of Fig. 1F.

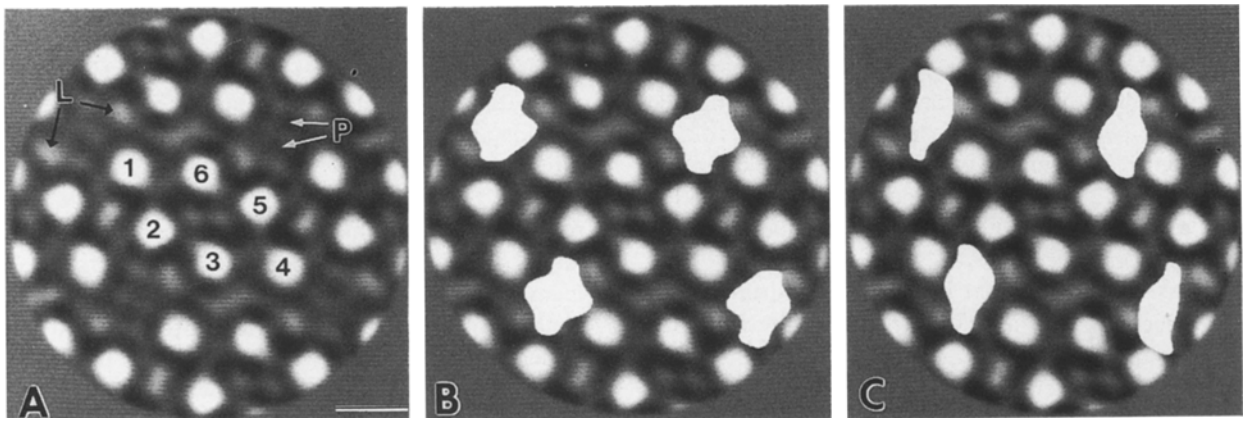

Fig. 2. Localization of peptide and cytochrome *c* binding sites on the VDAC array. (A) projected density map of crystalline VDAC obtained by cryo-electron microscopy of an unstained membrane. Bar = 5 nm. The six water-filled pore lumens in the central unit cell are numbered. Some of the low-density lipid domains and high-density protein "arms" at the unit cell corners are labelled "L" and "P," respectively. (B,C) Superposition on the VDAC crystal map of the zones of strongest negative stain exclusion from correlation averages of images of arrays incubated with apocytochrome *c* (B) and the cytochrome oxidase targeting peptide (C). Note the slight misalignment of the white zones in (C) with the frozen-hydrated map, due to the contraction of the lattice of the peptide-treated membrane (lattice angle equals 104° instead of 108°).

Mapping of the Stain-Exclusion Zones to the VDAC Protein

The white "s"-shaped features present in images of peptide-treated membrane crystals of the VDAC protein and absent from images of control specimens most likely correspond to positions at which the peptide accumulates on the array surface, thereby causing stain to be excluded to a much greater extent than usual. In order to identify the membrane component to which the targeting peptide binds, a map of the maximum stain-excluding zones in the correlation average of the peptide-treated array was aligned to and superimposed upon the projected density map of frozen-hydrated VDAC (obtained by cryo-electron microscopy; see Mannella *et al.*, 1989). The same procedure was also applied to the stain-exclusion map obtained in the previous study of cytochrome *c* binding to VDAC arrays (Mannella *et al.*, 1987) for purposes of comparison.

Figure 2A is a two-dimensional density map of frozen-hydrated crystalline VDAC. Note that the six pore lumens in the repeat unit of this array are white, since they are filled with water (the lowest density component of the arrays) instead of a heavy-metal-containing stain as in the images of Fig. 1. Each white lumen in Fig. 2A is surrounded by a thin, black rim of protein, the densest membrane component. The protein-lined pores are bounded, in turn, by patches of intermediate density that most likely correspond to lipid. (The area of these patches shrink when the lattices contract in response to extended phospholipase treatment; see Mannella *et al.*, 1986; Mannella, 1986). In addition, long dark (protein) "arms" extend into the lipid domains at each corner of the unit cell.

The inferred positions of apocytochrome *c* and the targeting peptide of subunit IV of cytochrome oxidase on the VDAC array are presented in Fig. 2B and 2C, respectively. Both the peptide and cytochrome *c* bind at the four corners of the unit cell, regions containing several low-density lipid patches that are criss-crossed by the lateral protein "arms." Careful comparison of the corner regions in the maps of Fig. 2 indicates that the stain-exclusion zones of both the cytochrome and the peptide coincide with the protein "arms," and not with the numerous domains of low-density lipid in the same vicinities. This suggests a specific interaction between the imported macromolecules and the VDAC protein.

DISCUSSION

The electron microscopic data presented above indicates that the targeting sequence of a cytochrome oxidase subunit and cytochrome *c* bind to the same specific site on membrane crystals of VDAC. In the case of the targeting sequence, this binding is associated with a structural change in the channel arrays —a disordering and contraction of the crystal lattice

—suggesting a significant interaction between the peptide and the membrane crystal. The only other macromolecule that induces a similar lateral phase transition in the VDAC crystal is the synthetic polyanion which modulates the channel's voltage dependence (Mannella and Guo, 1990; Colombini *et al.*, 1987). (The possibility that the targeting peptide may also alter VDAC's voltage dependence bears investigation.)

It is well known that both mitochondrial targeting sequences and apocytochrome *c* interact with phospholipids (e.g., Dumont and Richards, 1984; Tamm, 1986; Skerjanc *et al.*, 1987). The targeting sequences form amphiphilic α-helices in lipid environments (Roise *et al.*, 1986; Tamm and Bartoldus, 1990), and cytochrome *c* has amphiphilic α-helices at both N- and C-termini which are implicated in its binding to membranes (Jordi *et al.*, 1989; De Jongh and De Kruijff, 1990; Sprinkle *et al.*, 1990). Therefore, it is likely that both polypeptides bind to some extent to lipid domains present on the surface of the VDAC membrane crystals. However, since evidence for polypeptide-lipid attachment does not survive the averaging techniques employed in the present studies, such binding is probably sporadic and random. In other experiments (Mannella and Guo, unpublished), membrane crystals of bacteriorhodopsin (gift of B. A. Wallace) were incubated with the targeting peptide under conditions identical to those employed above. Stain-excluding filaments like those observed with the VDAC arrays were also seen on the purple membranes. However, the peptide fibers did not form periodic patterns on the bacteriorhodopsin arrays, nor were the lattice parameters of the arrays altered by the binding. These differences suggest a specificity in the interaction of the targeting peptide with membrane crystals of VDAC that is missing in its interactions with the other membrane.

The nature of the "arms" at the corners of the VDAC array to which the targeting peptide and cytochrome *c* bind is under investigation. One hypothesis (Mannella, 1990) is that each "arm" represents the N-terminal region of a VDAC polypeptide. That this is the case is suggested by results of preliminary experiments (Mannella and Guo, unpublished results) with antibodies raised against synthetic peptides corresponding to residues 1–20 of the *N. crassa* VDAC polypeptide. Fab fragments derived from these antibodies bind to the same corner region of the unit cell in the VDAC lattice as cytochrome *c* and the cytochrome oxidase targeting peptide. Interestingly, the N-terminal sequence of VDAC is, like the mitochondrial targeting sequences, predicted to form an amphiphilic α-helix (Kleene *et al.*, 1987). This raises the possibility that binding of the targeting peptide and cytochrome *c* to VDAC is via helix–helix interactions.

Do the above results have any relevance to the mechanisms by which proteins are recognized at and transported across the mitochondrial outer membrane? So far, various biochemical and molecular genetic approaches to identify mitochondrial components involved in protein import have not pointed to VDAC. In fact, it has been shown that yeast strains in which this pore's gene is disrupted are viable (Dihanich *et al.*, 1987), which might suggest that VDAC/porin is not involved in so fundamental a process as protein import. However, this conclusion is at best premature for at least two reasons:

1. It has been determined subsequently that another channel is overexpressed in VDAC-deficient mutants which, presumably, takes over some or all of VDAC's functions (Dihanich *et al.*, 1989).

2. In general, the picture that is developing for mitochondrial protein import is one of a complex machinery with considerable built-in redundancy (Hartl *et al.*, 1989; Baker and Schatz, 1991). For instance, fungal strains lacking individual putative precursor receptors are viable (Pfanner *et al.*, 1991).

In conclusion, the available biochemical evidence does not preclude the possibility that VDAC might serve as a component of one of the recognition and/or transport processes involved in mitochondrial protein uptake. On the contrary, the structural results presented here argue that the interactions between this mitochondrial channel and imported proteins warrant a closer look. In particular, the possibility of direct helix–helix interactions at the mitochondrial surface between the N-terminus of VDAC and the targeting sequences of imported proteins should be tested.

ACKNOWLEDGMENTS

The authors thank Li-Ming Chang Chien (amino acid composition and sequence of peptide), Bernard Cognon (electron microscopy), and Shangmin Yan (computer image processing) for expert technical assistance. We also thank Dr. Joachim Frank for helpful discussions in the course of this work and critical reading of this manuscript. This study was supported by National Science Foundation grants

DMB-8916315, PCM-8313045, and DIR-8914757 and NIH grant 1S15 GM4344301.

REFERENCES

Baker, K. P., and Schatz, G. (1991). *Nature (London)* **349,** 205–208.

Benz, R. (1985). *CRC Crit. Rev. Biochem.* **19,** 145–190.

Colombini, M. (1979). *Nature (London)* **279,** 643–645.

Colombini, M., Yeung, C. L., Tung, J., König, T. (1987). *Biochim. Biophys. Acta* **905,** 279–286.

De Jongh, H. H. J., and De Kruijff, B. (1990). *Biochim. Biophys. Acta* **1029,** 105–112.

De Pinto, V., Ludwig, O., Krause, J., Benz, R., and Palmieri, F. (1987). *Biochim, Biophys. Acta* **894,** 109–119.

Dihanich, M., Suda, K., and Schatz, G. (1987). *EMBO J.* **6,** 723–728.

Dihanich, M., Schmid, A., Oppliger, W., and Benz, R. (1989). *Eur. J. Biochem.* **181,** 703–708.

Dumont, M. E., and Richards, F. M. (1984). *J. Biol. Chem.* **259,** 4147–4156.

Frank, J. (1982). *Optik* **63,** 67–89.

Frank, J., Shimkin, B., and Dowse, H. (1981). *Ultramicroscopy* **6,** 343–358.

Freitag, H., Neupert, W., and Benz, R. (1982). *Eur. J. Biochem.* **123,** 629–639.

Glaser, S. M., and Cumsky, M. G. (1990). *J. Biol. Chem.* **265,** 8808–8816.

Goldfarb, W., Frank, J., Kessel, M., Jsung, J. C., Kim, C. H., and King, T. E. (1979). In *Cytochrome Oxidase* (King, T. E., Orii, Y., Chance, B., and Okunuki, K., eds.), Elsevier North-Holland Biomedical Press, Amsterdam, pp. 161–175.

Hartl, F. U., Pfanner, N., Nicholson, D. W., and Neupert, W. (1989). *Biochim. Biophys. Acta* **988,** 1–45.

Henry, J. P., Chich, J. F., Goldschmidt, D., and Thieffry, M. (1989). *J. Membr. Biol.* **112,** 139–147.

Holden, M. J., and Colombini, M. (1988). *FEBS Lett.* **241,** 105–109.

Jordi, W., De Kruijff, B., and Marsh, D. (1989). *Biochemistry* **28,** 8998–9005.

Kleene, R., Pfanner, N., Pfaller, R., Link, T., Sebald, W., Neupert, W., and Tropschug, M. (1987). *EMBO J.* **6,** 2627–2633.

Lemire, B. D., Fankhauser, C., Baker, A., and Schatz, G. (1989). *J. Biol. Chem.* **264,** 20206–20215.

Mannella, C. A. (1984). *Science* **224,** 165–166.

Mannella, C. A. (1986). *Methods Enzymol.* **125,** 595–610.

Mannella, C. A. (1989). *J. Bioenerg. Biomembr.* **21,** 427–437.

Mannella, C. A. (1990). *Experientia* **46,** 137–145.

Mannella, C. A., and Guo, X. W. (1990). *Biophys. J.* **57,** 23–31.

Mannella, C. A., Ribeiro, A. J., and Frank, J. (1986). *Biophys. J.* **49,** 307–318.

Mannella, C. A., Ribeiro, A. J., and Frank, J. (1987). *Biophys. J.* **51,** 221–226.

Mannella, C. A., Guo, X. W., and Cognon, B. (1989). *FEBS Lett.* **253,** 231–234.

Pfanner, N., Söllner, T., and Neupert, W. (1991). *Trends Biochem. Sci.* **16,** 63–67.

Roise, D. (1988). *Prog. Clin. Biol. Res.* **282,** 43–53.

Roise, D., Horvath, S. J., Tomich, J. M., Richards, J. H., and Schatz, G. (1986). *EMBO J.* **5,** 1327–1334.

Roise, D., Theiler, F., Horvath, S. J., Tomich, J., Richards, J. H., Allison, D. S., and Schatz, G. (1988). *EMBO J.* **7,** 649–653.

Sachs, M. S., David, M., Werner, S., and RajBhandary, U. L. (1986). *J. Biol. Chem.* **261,** 869–873.

Saxton, W. O. (1980). In *Electron microscopy at molecular dimensions* (Baumeister, W., and Vogell, W., eds.), Springer-Verlag GmbH and Co., KG, Berlin, pp. 244–255.

Skerjanc, I. S., Shore, G. C., and Silvius, J. R. (1987). *EMBO J.* **6,** 3117–3123.

Sprinkle, J. R., Hakvoort, T. B. M., Koshy, T. I., Miller, D. D., and Margoliash, E. (1990). *Biochemistry* **87,** 5729–5733.

Tamm, L. K. (1986). *Biochemistry* **25,** 7470–7476.

Tamm, L. K., and Bartoldus, I. (1990). *FEBS Lett.* **272,** 29–33.

Von Heijne, G. (1986). *EMBO J.* **5,** 1335–1342.